

Collective vibration of discharge current filaments in a self-organized pattern within a dielectric barrier discharge

Lifang Dong, Jie Shang, Yafeng He, Zhanguo Bai, Liang Liu, and Weili Fan
College of Physics Science and Technology, Hebei University, Baoding 071002, China
and Hebei Key Laboratory of Optic-electronic Information Materials, Baoding 071002, China

(Received 4 November 2011; published 18 June 2012)

We report on the collective vibration of discharge current filaments in a self-organized superlattice pattern within an air-argon dielectric barrier discharge system. The period of collective vibration decreases as the air content increases. An antisymmetric normal vibration mode of discharge current filaments is observed. The measurements of the spatiotemporal behavior of the superlattice pattern show that the discharge of the vibrating dot (filament) is asynchronous with that of its eight neighboring dots, including four big dots and four small dots. The forces exerted on the vibrating dot are analyzed, and a motion equation is set up in each half cycle of the applied voltage. It is found that the motion of the small dot is not an ideal vibration but is a vibration with fluctuating amplitude, which is in good agreement with experiments.

DOI: [10.1103/PhysRevE.85.066403](https://doi.org/10.1103/PhysRevE.85.066403)

PACS number(s): 52.80.Tn, 47.54.-r, 89.75.Kd

The collective phenomenon as a kind of universal phenomenon has been researched in various fields, such as physics, chemistry, biology, engineering, and so on [1–9]. In recent years, a topic of high interest has been the collective phenomenon in the dielectric barrier discharge (DBD) system [10–22]. In particular, self-organization and the interaction of filaments have become the focus. At present, two types of self-organization, a stationary filament pattern and wholly moving filament pattern, have been observed [11–22]. However, to the best of our knowledge, there has not been a report on the collective motion of discharge current filaments interleaved in a self-organized stationary current filament lattice.

In this paper, we report an observation on collective vibration in a self-organized complex superlattice pattern within a dielectric barrier discharge system. The vibration mode of discharge current filaments and the spatiotemporal behavior of the superlattice pattern are investigated. The forces exerted on the vibrating dot are analyzed, and a motion equation is set up in each half cycle of the applied voltage.

Figure 1 shows a schematic of the experimental setup. Two cylindrical containers with a diameter of 75 mm, sealed with 1.5 mm thick glass plates, are filled with water. Two metallic rings are immersed in water in the two containers and are connected to an ac power supply with a driving frequency of 55 kHz. Thus, the water acts as a liquid electrode that is electrically conductive, well thermally stable, and transparent. The glass plates serve as dielectric layers, and a hexagonal glass frame with a thickness of 2.0 mm and a length of 2.5 cm is placed between the two parallel glass plates, serving as the lateral boundary. The entire apparatus is enclosed in a chamber filled with an air-argon mixture at 1 atm pressure. The amplitude of the driven voltage can be measured by a high-voltage probe (Tektronix P6015A 1000X). The light emitted from different discharge current filaments is detected by two lens-aperture photomultiplier tube (PMTs, RCA 7265) systems and recorded by an oscilloscope (Tektronix TDS3054B, 500 MHz) simultaneously. A digital camera (Konica Minolta Dimage Z2) is used to record the images of patterned discharges.

Figure 2 shows that the vibrating hexagonal superlattice pattern consists of two types of spots (filaments), large steady

spots and small vibrating spots, which present dots at a short exposure time and sticks at a long exposure time. In order to get the vibration period T , a series of snapshots with different exposure times were taken and analyzed. The vibration period of the small dot is determined by measuring the variation of the motion trace length L as a function of exposure time. Obviously, the length of the motion trace increases with the exposure time to its maximum (twice the amplitude of the vibration), and then it remains constant. In one period the type of increase is in different stepladder depending on the beginning position of the small dot when the camera shutter is opened. If the motion of the small dots is an ideal vibration where the equilibrium position and the amplitude remain unchanged, the time at which the length of the motion trace starts to become constant will be in the range of $0.5T$ to T .

In fact, it is hard to observe the stepladder increase in the motion trace length of a small dot because the exposure time is discrete and the motion trace length of a small dot at a certain exposure time is the statistical average value over all small dots in experiments. As shown in Fig. 3(a), it is found that L first increases (A-B, 10–16.7 ms) and then approximately remains constant for a while (B-C, 16.7–20 ms). As analyzed above, the vibration period should be in the range of 16.7–33.4 ms. After approximately remaining at a constant length, L shows a further increase (C, 20 ms). As mentioned above, L is the statistical average value over all small dots; thus there must be a portion of small dots whose motion trace length is larger than the average value. If the exposure time is not longer than one vibration period, almost all motion trace lengths remain constant, and a few increase with exposure time. So L presents as approximately remaining constant for a while (B-C, 16.7–20 ms). If the exposure time exceeds one period, the fraction of increasing trace lengths will significantly increase, maybe due to the fluctuation of the vibration amplitude. Therefore L shows a further increase after remaining constant. Thus the vibration period is approximately set as exposure time C (20 ms), at which the trace length further increases, with an error of the difference between C and B (3.3 ms).

Figure 3(b) gives the variations of the vibration period and the applied voltage as a function of air content. It is found that the vibration period decreases with increasing air

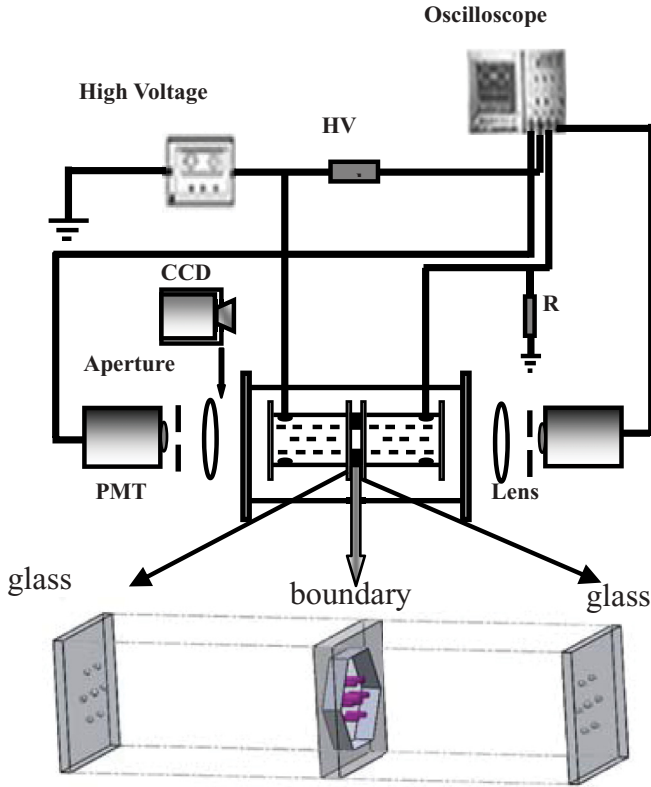


FIG. 1. (Color online) Schematic of the experimental setup.

content, while the applied voltage for the pattern formation increases.

Figure 4 gives the vibration mode of the vibrating hexagonal superlattice pattern. The circled cell in Figs. 4(a) and 4(b) show the maximum displacement and the equilibrium position of the vibration, respectively. Figure 4(d) gives the spatial intensity distributions along line A (or B or C) in Fig. 4(c). The alternation of a short interval and long one in Fig. 4(d) indicates that the small dots in line A (or B or C) in Fig. 4(c) move along the same direction. Based on the above results, a schematic diagram of the vibration mode is given in Fig. 4(e), in which the direction of the arrows denotes the direction of the movement of the small spots. Six small spots in one cell are divided into two groups to form two triangles; one moves inward while the other one moves outward to keep the center of mass immovable. This is an antisymmetric normal vibration mode [23].

In order to explore the interaction between discharge current filaments, which results in the vibration of the small dots, the correlations between any two spots in the vibrating hexagonal superlattice pattern are measured and are shown in Fig. 5. It is found that small dots with same sign in Fig. 6 volley at the edge where $\frac{d|U|}{dt} > 0$, which is referred to as the rising edge of the applied voltage in the following [Fig. 5(a)], while dots with different signs do not discharge simultaneously [Fig. 5(b)]. Figure 5(c) shows that all the large dots are ignited synchronously two times, one at the rising edge and the other at the edge where $\frac{d|U|}{dt} < 0$, which is referred to as the falling edge of the applied voltage in the following, in each half cycle of the applied voltage. As shown in Fig. 5(d), the sequence of any small spot sublattice (S) and the large spot sublattice (L)

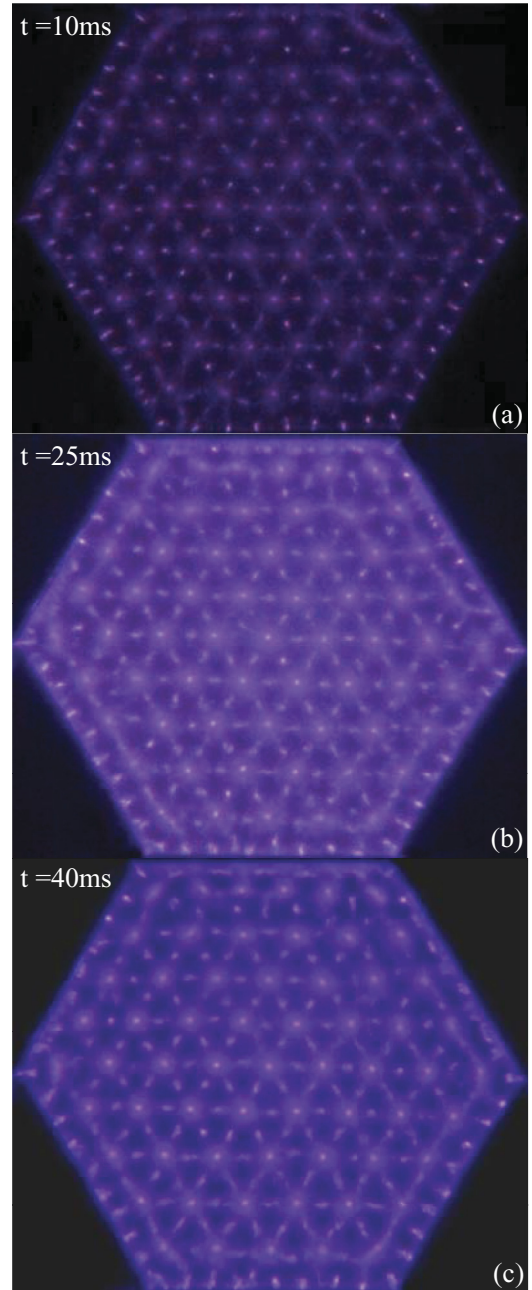


FIG. 2. (Color online) Images of the vibrating hexagonal superlattice pattern with different exposure times, (a) $t = 10$ ms, (b) 25 ms, and (c) 40 ms.

is S-L-L in each half cycle of the applied voltage. Figure 6 gives a schematic diagram of the spatiotemporal structure of the vibrating hexagonal superlattice pattern, in which the dots with same sign discharge simultaneously while the dots with different signs do not.

As is well known, there are two kinds of forces between two filaments: the Lorentz force when they discharge simultaneously and the Coulomb force between wall charges [21]. According to the above studies, the vibrating small dot and its eight neighboring dots (four big dots and four small dots) do not discharge simultaneously, so the forces exerted on the vibrating dot are the Coulomb force.

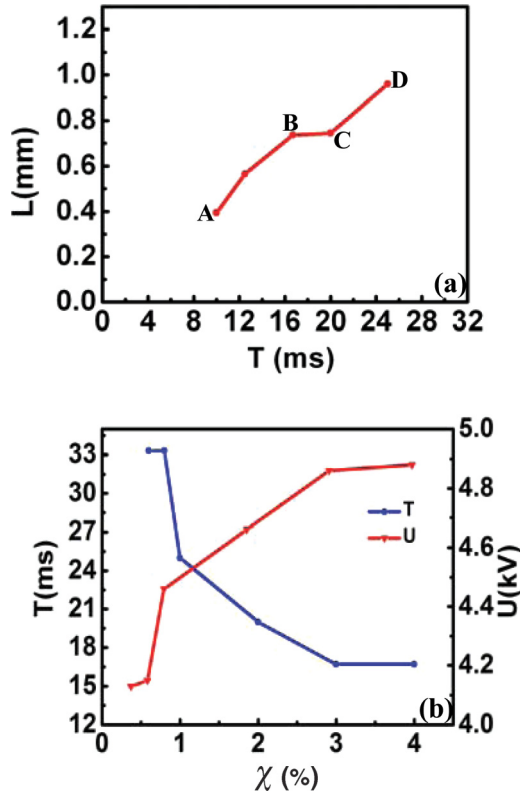


FIG. 3. (Color online) (a) The variation of the motion trace length L as a function of exposure time, $\chi = 2\%$, $P = 1$ atm. (b) The variations of the vibration period T and the applied voltage for vibrating hexagonal pattern formation U with air content χ .

The measurements on the spatiotemporal behavior of the superlattice pattern show that there are five discharges in one half cycle of the applied voltage. The first three correspond to the ignition of three sets of small dots at the rising edge ($\frac{d|U|}{dt} > 0$). Then the big dots discharge twice, one at the rising edge and the other at almost zero applied voltage in the falling

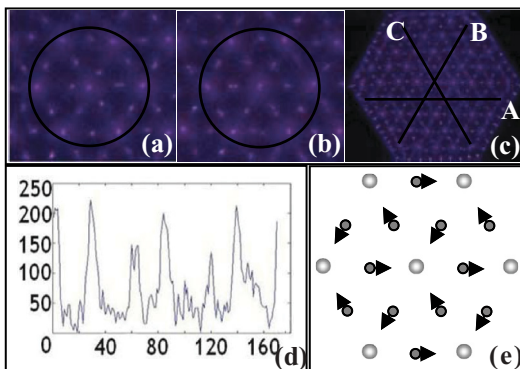


FIG. 4. (Color online) The vibration mode of the vibrating hexagonal superlattice pattern. (a)–(c) Pictures of the vibrating hexagonal superlattice pattern at an exposure time of 10 ms. (d) The spatial intensity distributions along line A (or B or C) in (c). (e) A schematic diagram of the vibration mode, which is deduced from (a)–(d). The circled cells in (a) and (b) show the maximum displacement and the equilibrium position of the vibration, respectively.

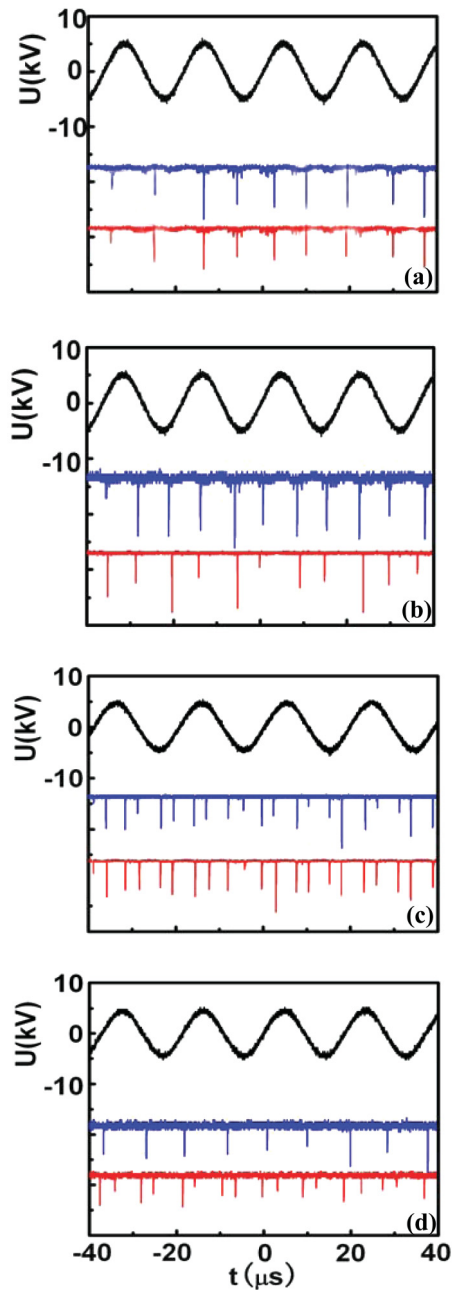


FIG. 5. (Color online) (a) The light signal of two small dots with same sign. (b) The light signal of two small dots with different signs. (c) The light signal of two big dots. (d) The light signal of a small dot and a big dot.

edge ($\frac{d|U|}{dt} < 0$), which is driven by the field produced by wall charges deposited on the last discharge. When the wall charges are nearly exhausted, the discharge extinguishes.

Figure 7 shows a schematic diagram of the force analysis on the vibrating small dot. In order to analyze the forces exerted on the vibrating dot, each half cycle of the applied voltage is roughly divided into two zones according to the discharge stages of the big dots: the first one is the range from the moment of the first discharge of the big dots at the rising edge to that of the second discharge at the falling edge; the second one is the range from the moment of the end of the second discharge

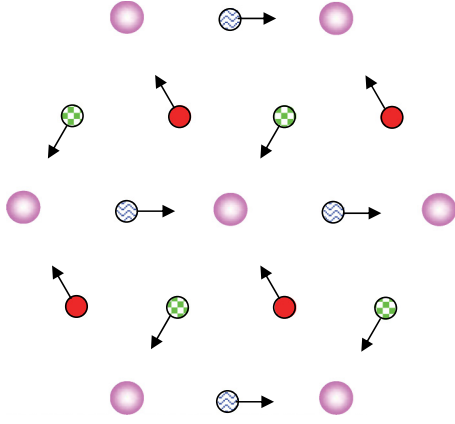


FIG. 6. (Color online) Schematic diagram of the interleaving of four sets of sublattices denoted by different signs of the vibrating hexagonal superlattice pattern. The spatiotemporal evolution is S-L-L-S-L-L in one cycle of applied voltage. Arrows show the vibrations of each small spot in the vibrating hexagonal superlattice pattern.

of the big dots at the falling edge to that of the discharge at the next rising edge.

In the first zone, the Coulomb force between any two dots is repulsive as they have same wall charge sign. Considering that the Coulomb force is dependent upon the charges of two dots and the distance between two dots, the forces exerted on the vibrating dot by its neighboring dots, including four big dots and four small dots, are given schematically in Fig. 7(a), in which the arrows show the direction and magnitude of the forces. Then the resultant force $\sum_{i=1}^8 F_i$ exerted on the vibrating small dot by eight dots is found to point to its equilibrium position along the direction of L_1 -S- L_2 .

In the second zone, the charge of the big dots is almost zero after they discharge at the falling edge, so the forces exerted on the vibrating dot mainly come from four neighboring small dots. The direction of the resultant force $\sum_{i=1}^8 F_i$ is also along L_1 -S- L_2 , but its magnitude is almost zero in Fig. 7(b).

Based on above force analysis in Fig. 7, by using the first-order Taylor expansion of the resultant force, the motion of the vibrating dot is approximately described by

$$\begin{aligned} \frac{d^2 r}{dt^2} &= -\kappa r, & t_1 + n \frac{T_v}{2} \leq t \leq t_2 + n \frac{T_v}{2}, \\ \frac{d^2 r}{dt^2} &\approx 0, & t_2 + n \frac{T_v}{2} \leq t \leq t_1 + (n+1) \frac{T_v}{2}, \end{aligned}$$

where the center of two big dots (the equilibrium position) is set as the origin, r is the distance away from the equilibrium position of the vibrating small dot, t_1 and t_2 are the discharge moment of the big dot at the rising and falling edges, respectively, and T_v is the driving cycle of the applied voltage.

From the above equations, the motion of the small dot is not an ideal vibration. It should be a vibration with fluctuating amplitude, which results from the approximate uniform motion. It is in agreement with the experimental results in following two aspects: one is that the trace length will further increase after one vibration period, and the other is that not all of the small dots can experience a perfect triangle as in Fig. 4(a). Obviously, in one vibrating

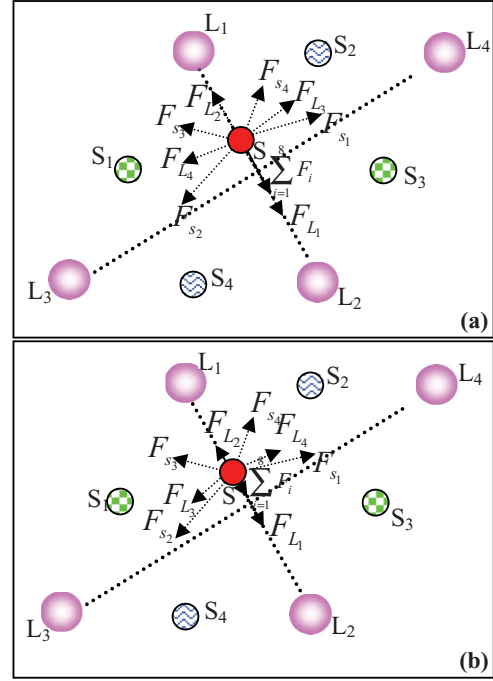


FIG. 7. (Color online) Schematic diagrams of forces exerted on one vibrating dot by its neighboring dots, including four big dots and four small dots in two different situations. (a) Force analysis on the vibrating small dot during the time interval between the discharge moment of big spots at the rising edge and that at the falling edge. (b) Force analysis on the vibrating small dot during the time interval between the moment of the end of the second discharge of the big dots at the falling edge and that at the next rising edge. In each diagram, F_{L_i} , F_{S_i} , and $\sum_{i=1}^8 F_i$ are the forces exerted by a big dot, the forces exerted by a small dot, and the resultant force, respectively.

period (millisecond scale) the small dot experiences many alternations between acceleration or deceleration ($t_1 + n \frac{T_v}{2} \leq t \leq t_2 + n \frac{T_v}{2}$, microsecond scale) and approximate uniform motion [$t_2 + n \frac{T_v}{2} \leq t \leq t_1 + (n+1) \frac{T_v}{2}$, microsecond scale]. The approximate uniform motion results in the fluctuation of the amplitude of the vibration; that is, the amplitude may decrease, remain constant, or increase in the next period of the vibration. The trace length remains constant if the amplitude is reduced or unchanged, but it increases if the amplitude has a positive fluctuation. As mentioned above, the trace length obtained in experiments is the statistical average value over all small dots in the superlattice pattern. There must be a portion of small dots whose amplitudes increase compared to the average value. The fraction of increasing trace lengths will increase due to the fluctuation of the vibration amplitude, which results in the trace length further increasing after one period. Based on the above analysis, the trace length further increases after one vibration period; thus the moment at which the trace length increases further after remaining constant can be determined as the vibration period of the small dots. It is worth pointing out that the above model is very approximate for simplicity. In future work, the collective vibration of small dots will be further researched by considering the interaction between discharge filaments in detail.

In conclusion, the collective vibration of discharge filaments in a self-organized superlattice pattern within a dielectric barrier discharge system was observed. An asymmetrical vibration mode was found. The spatiotemporal behavior of the superlattice pattern was investigated. It was found that the vibrating dot and its eight neighboring dots (four big dots and four small dots) do not discharge simultaneously. The forces exerted on the vibrating dot by the eight neighboring dots were analyzed. According to the force analysis, an approximate model of the vibrating dot was set up. It was found that the motion of the small dot is not an ideal vibration but a vibration with fluctuating amplitude. This result is in good agreement with the experimental results in the following two aspects: one is that the trace length will further increase after one vibration

period, and the other is that not all of the small dots can experience a perfect triangle. The results will promote the research of the collective phenomenon and interaction in a gas discharge.

This work is supported by the National Natural Science Foundation of China under Grant No. 1175054, the Natural Science Foundation of Hebei Province, China, under Grant No. A2010000185, the Research Foundation of the Education Bureau of Hebei Province, China, under Grant No. ZD2010140, the Key basic research project in the application basic research plan of Hebei Province under Grant No.11967135D, and the Specialized Research Fund for the Doctoral Program of Higher Education, State Education Ministry of China (Grant No. 20101301110001)

-
- [1] Z. L. Chen, J. G. Bohnet, S. R. Sankar, J. Dai, and J. K. Thompson, *Phys. Rev. Lett.* **106**, 133601 (2011).
 - [2] N. Coq, A. Bricard, F. D. Delapierre, L. Malaquin, O. duRoure, M. Fermigier, and D. Bartolo, *Phys. Rev. Lett.* **107**, 014501 (2011).
 - [3] D. A. Abanin and D. A. Pesin, *Phys. Rev. Lett.* **106**, 136802 (2011).
 - [4] W. Rother *et al.*, *Phys. Rev. Lett.* **106**, 022502 (2011).
 - [5] Y. Y. Jung, M. N. Slipchenko, C. H. Liu, A. E. Ribbe, Z. Zhong, C. Yang, and J. X. Cheng, *Phys. Rev. Lett.* **105**, 217401 (2010).
 - [6] T. Ishikawa, N. Yoshida, H. Ueno, M. Wiedeman, Y. Imai, and T. Yamaguchi, *Phys. Rev. Lett.* **107**, 028102 (2011).
 - [7] R. Candelier and O. Dauchot, *Phys. Rev. Lett.* **103**, 128001 (2009).
 - [8] S. G. Clark and A. S. Parkins, *Phys. Rev. Lett.* **90**, 047905 (2003).
 - [9] A. Zemel, I. B. Bischofs, and S. A. Safran, *Phys. Rev. Lett.* **97**, 128103 (2006).
 - [10] U. Kogelschatz, *J. Phys.* **257**, 012015 (2010).
 - [11] J. Guikema, N. Miller, J. Niehof, M. Klein, and M. Walhout, *Phys. Rev. Lett.* **85**, 3817 (2000).
 - [12] W. Breazeal, K. M. Flynn, and E. G. Gwinn, *Phys. Rev. E* **52**, 1503 (1995).
 - [13] M. Klein, N. Miller, and M. Walhout, *Phys. Rev. E* **64**, 026402 (2001).
 - [14] L. Dong, W. Liu, H. Wang, Y. He, W. Fan, and R. Gao, *Phys. Rev. E* **76**, 046210 (2007).
 - [15] X. X. Duan, J. T. Ouyang, X. F. Zhao, and F. He, *Phys. Rev. E* **80**, 016202 (2009).
 - [16] L. F. Dong, R. L. Gao, Y. F. He, W. L. Fan, and W. W. Liu, *Phys. Rev. E* **74**, 057202 (2006).
 - [17] A. L. Zanin, E. L. Gurevich, A. S. Moskalenko, H. U. Bodeker, and H.-G. Purwins, *Phys. Rev. E* **70**, 036202 (2004).
 - [18] I. Muller, C. Punset, E. Ammelt, H.-G. Purwins, and J. P. Boeuf, *IEEE Trans. Plasma Sci.* **27**, 20 (1999).
 - [19] L. Stollenwerk, J. G. Laven, and H.-G. Purwins, *Phys. Rev. Lett.* **98**, 255001 (2007).
 - [20] L. Stollenwerk, Sh. Amiranashvili, J.-P. Boeuf, and H.-G. Purwins, *Phys. Rev. Lett.* **96**, 255001 (2006).
 - [21] T. Shirafuji, T. Kitagawa, T. Wakai, and K. Tachibana, *Appl. Phys. Lett.* **83**, 12 (2003).
 - [22] M. Schwabe, U. Konopka, P. Bandyopadhyay, and G. E. Morfill, *Phys. Rev. Lett.* **106**, 215004 (2011).
 - [23] A. Melzer, M. Klindworth, and A. Piel, *Phys. Rev. Lett.* **87**, 115002 (2001).